Advances in carbon-based composite anodes with gradients of lithiophilicity and conductivity used for stable lithium metal batteries

WANG Ya-nan[1,2], ZHAN Ying-xin[1,2], ZHANG Xue-qiang[1,*], HUANG Jia-qi[1]

（1. *Advanced Research Institute of Multidisciplinary Science*, *Beijing Institute of Technology*, *Beijing* 100081, *China*;
2. *School of Materials Science and Engineering*, *Beijing Institute of Technology*, *Beijing* 100081, *China*）

Abstract: To address the issues of non-uniform Li plating/stripping and the large volume fluctuations during their repeated cycling, Li metal anodes, a composite Li anode with a three-dimensional (3D) host has been proposed as a promising strategy to improve the uniformity of Li plating/stripping and relieve volume fluctuations. One key strategy in this area is to develop 3D carbon hosts with gradients of lithiophilicity and conductivity to guide Li deposition from bottom to top, thus maximizing the positive effect of this composite Li anode. Such anodes have recently received significant attention due to the flexibility, adjustability, (electro)chemical stability and light weight of the carbon hosts. This review summarizes recent advances in these anodes, categorizing them into those that have hosts with a lithiophilicity gradient, hosts with a conductivity gradient, and those that have both. Latest research findings are discussed and these different anode categories are reviewed. Prospects for the design of such anodes to promote the use of Li metal anodes in high-energy-density rechargeable batteries are presented.

Key words: Lithium metal battery; Composite lithium anode; Gradient lithiophilicity; Gradient conductivity; Dual gradient

1 Introduction

Rapid development of portable electronic devices and electric vehicles has prompted the exploration of high-energy-density batteries[1–3]. Lithium (Li)-ion batteries have profoundly shaped our daily life by developing a non-fossil and wireless world[4–7]. The energy density of Li-ion batteries increases from about 90 to 270 Wh kg^{-1} after the development of more than 30 years since 1991[8–12]. Nevertheless, the energy density of Li-ion batteries is approaching the ceiling (< 350 Wh kg^{-1}) limited by the intercalation mechanism of the anode and cathode[13–15]. In order to further improve the energy density of batteries, Li metal anode is reviving for its high theoretical specific capacity (3860 mAh g^{-1}) and low electrode potential (−3.04 V vs. standard hydrogen electrode)[16–20]. The research of Li metal anodes in batteries began in the 1960s[21–22]. In the 1980s, secondary Li metal batteries were commercialized by Moli Energy Company even though they failed[23–24]. The main obstacle on the way to practical Li metal anodes is non-uniform Li plating/stripping accompanied by large volume fluctuations, which results in low Coulombic efficiency (CE) and short lifespan of Li metal batteries[25–28]. Furthermore, the growth of Li deposition in the form of dendrites could pierce the separator and induce battery safety concerns[29–32]. Despite the above challenges, the high energy density (> 400 Wh kg^{-1}) of Li metal batteries is still attractive and competitive. Therefore, improving the uniformity of Li deposition and mitigating volume fluctuations during cycles are under intensive research to stabilize Li metal anodes.

Tremendous efforts have been devoted to improving uniformity of Li deposition and mitigating volume fluctuations, such as liquid electrolyte design[33–38], artificial coating[39–44], lithiophilic sites[45–50], solid-state electrolytes[51–55] and composite Li anodes[56–61]. Among these strategies, a composite Li anode which employs a stable three-dimensional (3D) host emerges as a promising strategy for stabilizing Li metal anodes[62]. The large specific surface area of a 3D host could remarkably reduce local current density, thus mitigating the formation of Li dendrites based on Sand's time model[63–65]. Surface modification of a host, such as decorating with lithiophilic sites, could further improve the uniformity of Li de-

Received date: 2023-04-06; **Revised date:** 2023-05-29

Corresponding author: ZHANG Xue-qiang, Associate professor. E-mail: zhangxq@bit.edu.cn;
Author introduction: WANG Ya-nan. E-mail: 3120222013@bit.edu.cn

position in addition to the notable decrease in local current density[66–68]. Furthermore, the porous structure of a 3D host could provide space to effectively accommodate Li deposition and the formation of inactive Li, which contributes to relieving the volume fluctuations of composite Li anodes[69–71].

Generally, composite Li anodes with high electrical conductivity outperform those with low electrical conductivity and there is nearly no difference in electrical conductivity between the top and bottom of a host[72]. Once a Li ion contacts the host, it could obtain an electron rapidly. However, the diffusion of Li ions in bulk electrolytes is relatively slower than that of electrons in a host[73]. When the Li ions inside a host or near the surface of a host are consumed rapidly or even depleted, there is a concentration difference of Li ions between bulk electrolyte and electrode surface[74–76]. Then, the diffusion of Li ions from bulk to the surface is driven. When supplemental Li ions reach the top surface of a host, Li is inclined to deposit on the top surface which impedes subsequent Li deposition inside the host[77–78]. The porous structure of a host could not be utilized fully. Thus, inactive Li also inclines to form and accumulate on the top surface of a host, resulting in the rapid increase of polarization and deteriorating stability of composite Li anodes[79–80]. When it comes to practical Li metal batteries, a high cycling capacity (> 4.0 mAh cm^{-2}), limited Li (< 10.0 mAh cm^{-2}), and lean electrolytes (< 3.0 g Ah^{-1}) are indispensable for achieving high energy density at a cell level, which aggravates the selective Li deposition and accumulation of inactive Li on the top surface of composite Li anodes[81].

Gradient composite Li anodes are consequently proposed in order to guide the bottom-up deposition pattern of Li in a host. The difference in lithiophilicity and electrical conductivity between the top and bottom area of a host is designed to guide bottom-up Li deposition[82]. Remarkable progress has been made designing gradient composite Li anodes recently, which improves the utilization efficiency of a host. The design of gradient composite Li anodes emerges as a promising solution to improve the stability of composite Li anodes[83]. To further guide the rational design of gradient composite Li anodes, the systematic analysis of gradient composite Li anodes design is necessary.

In this review, advances in carbon-based gradient composite anodes for stable Li metal batteries were summarized (Fig. 1). In retrospect, various composite Li anodes have been developed, of which carbon-based composite Li anodes are favorable due to the flexible adjustability, (electro)chemical stability and light weight of carbon hosts[84–87]. Numerous carbon materials, such as carbon fiber, carbon nanotube and graphene, have been employed as the 3D hosts for composite Li anode preparations[88–92]. The gradient hosts could be categorized into gradient lithiophilicity, gradient conductivity and dual gradient, which are introduced in the following sections, respectively[93]. In addition, the relationship between gradient host structure and Li plating/stripping behavior is discussed. The merits and limitations of different gradient host structures are pointed out. Perspectives of rational designs on gradient composite Li anodes are further proposed to promote the practical applications of Li metal batteries.

2 Gradient composite Li anodes

2.1 Gradient lithiophilicity

Lithiophilic sites have a strong affinity with Li atoms or ions, which could facilitate uniform Li deposition[94–95]. The lithiophilicity mentioned here can

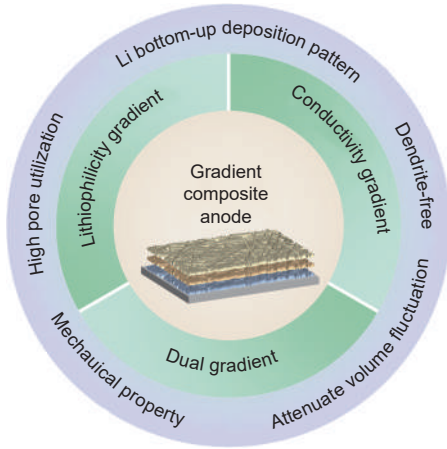

Fig. 1 Advantages and schematic diagram of the gradient composite anodes with lithiophilicity gradient, conductivity gradient and dual gradient

be categorized into 2 types according to the action object. One type is the ion–dipole interaction between Li ions and the polar functional groups on the surface of hosts, which guides lithiophilic sites to adsorb Li ions, such as carbide and doped carbon materials. The other type is that Li atoms will react with the lithiophilic sites on the surface of a host to reduce the Li nucleation barriers, such as metal and metal oxides. The rationale of gradient lithiophilic composite Li anodes is to decorate lithiophilic sites at the bottom of a host and decorate lithiophobic sites at the top of a host, so that the affinity for Li atoms or ions from bottom to top of the host is constantly reduced, forming gradient lithiophilicity inside the host. Gradient lithiophilic host can guide Li ions to preferentially nucleate and deposit at the bottom, thus avoiding deposition of Li at the top of the host.

Zhang et al. developed a host by sequentially dripping carbon nanotubes (CNTs) suspensions with gradient decreased concentrations of zinc oxide (ZnO) layer-by-layer on Li foil (GZCNT) (Fig. 2a-b)[96]. The gradient loading of ZnO from bottom to top serves as gradient lithiophilic sites inside GZCNT host. The bottom layer of lithiophilic ZnO/CNT is tightly anchored to Li foil, which facilitates the formation of stable solid electrolyte interphase (SEI) and inhibits Li corrosion. The top layer of lithiophobic CNT facilitates Li ion diffusion and provides mechanical strength to avoid Li dendrites. In a symmetric Li//Li pouch cell with a surface area of 10 cm^2, the GZCNT-coated Li anode maintained stable for over 200 cycles without any dendrites, while the voltage of bare Li anode fluctuated after 55 cycles (Fig. 2c). This strategy could enhance cycling stability of copper (Cu) current collector, 10 cm^2 Li foil pouch cell, and Li-sulfur (Li-S) battery significantly.

Yan et al. obtained a gradient lithiophilic 3D conductive host (GSCP) *via* magnetron sputtering of silicon (Si) on the bottom of a porous carbon paper (CP)[97]. The content of lithiophilic Si decreases from bottom to top due to unidirectional sputtering, forming a gradient lithiophilic host. Therefore, Li preferentially nucleates and grows in a bottom-up pattern and the space utilization of the host is elevated. GSCP anode maintained an average CE of 99.0% over 400 cycles in a Li//GSCP cell at 1.0 mA cm^{-2} and 1.0 mAh cm^{-2}, displaying excellent electrochemical reversibility. When the current density was increased to 5.0 mA cm^{-2}, the average CE of GSCP was 97.0% over 150 cycles. Before assembling the full cell, 5.0 mAh Li was deposited on a GSCP anode to obtain GSCP@Li anode. Matched with $Li_4Ti_5O_{12}$ (LTO, with a loading of ~1.2 mg cm^{-2}) cathode, GSCP@Li//LTO full cell delivered a specific capacity of 114.8 mAh g^{-1} at 10 C with capacity retention of 84.5% after 5 000 cycles.

The combination of carbon-based gradient lithiophilic host and modified lithiophilic substrate can effectively improve the efficiency of Li deposition. Yun et al. proposed a carbon host derived from metal-or-

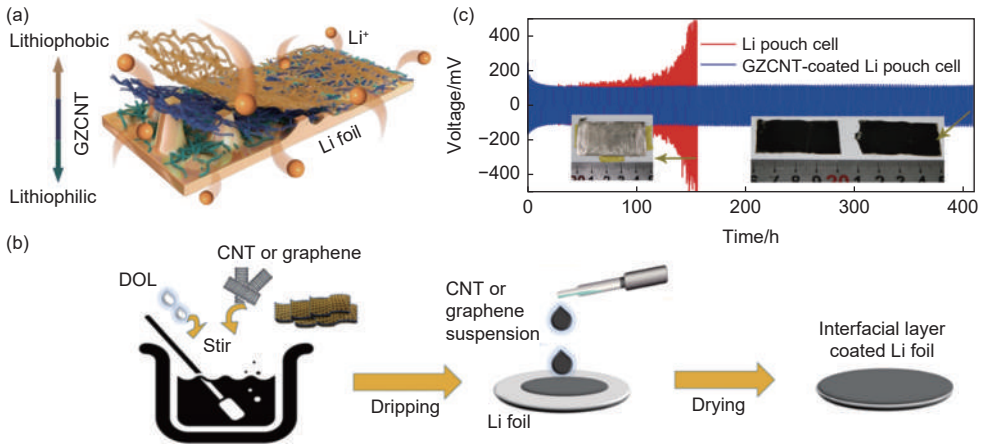

Fig. 2　(a) Schematic diagram of the GZCNT host-coated Li foil[96]. (b) Fabrication of interfacial layer of GZCNT. (c) Cycling performance of symmetric pouch cells. Inset: digital photograph of Li foil, and GZCNT-coated Li foils in pouch cells after 100 and 200 cycles, respectively. (Reprinted with permission)

ganic framework (MOF), which consisted of MOF-derived carbon (MOF-C) and Cu substrate modified with silver (Ag) layer (Cu@Ag)[98]. The electrodes with different thicknesses (*t*, μm) and substrates (X) were denoted as MOF-C(*t*)/X. To explore Li plating behavior, the voltage profiles of MOF-C(*t*)/X//Li pouch cells illustrated that MOF-C(30)/Cu@Ag electrode showed the lowest nucleation overpotential (6 mV), while the nucleation overpotential of MOF-C(30)/Cu was the highest (21 mV), illustrating Cu@Ag substrate could reduce barriers for Li nucleation. In the initial stage of deposition, Li ions reacted with Ag layer at the bottom of MOF-C(30)/Cu@Ag, which could regulate the subsequent Li deposition process. Experimental and simulation results indicated that local current density was the highest at the bottom of MOF-C(30)/Cu@Ag electrode and decreased upward, which suggested Li preferentially deposited at the bottom (Fig. 3a-b). However, when the thickness of MOF-C increased to 90 μm, the local current density was higher at the top than that at the bottom of MOF-C(90)/Cu@Ag electrode, because the ion transport resistance increased with the thickness increase of electrode. Thus, lithiophilic Cu@Ag substrate with high thickness above to 90 μm could lose its advantage of inhibiting top deposition (Fig. 3c). In MOF-C(*t*)/X//Li pouch cells, 2.0 mAh cm^{-2} of Li was prestored before the cycling tests, and the MOF-C(30)/Cu@Ag electrode exhibited stable cycling for over 250 cycles (500 h) at 0.4 mA cm^{-2} and 0.4 mAh cm^{-2} (Fig. 3d).

Graphene oxide (GO) is widely considered as a carbon host due to its excellent lithiophilicity. Some surface groups of reduced GO (rGO) have high binding energy to Li, indicating high surface lithiophilicity[99]. Nevertheless, tortuous and long Li ion transport pathways induce large transport impedance, and Li tends to be deposited at the upper area of the host. As a consequence, the anode with an aligned structure could provide low tortuosity Li ion transport pathways, leading to Li bottom-up deposition[100–101]. Hence, Ni et al. combined GO with aligned structure by 3D printing, and then infused molten Li to form

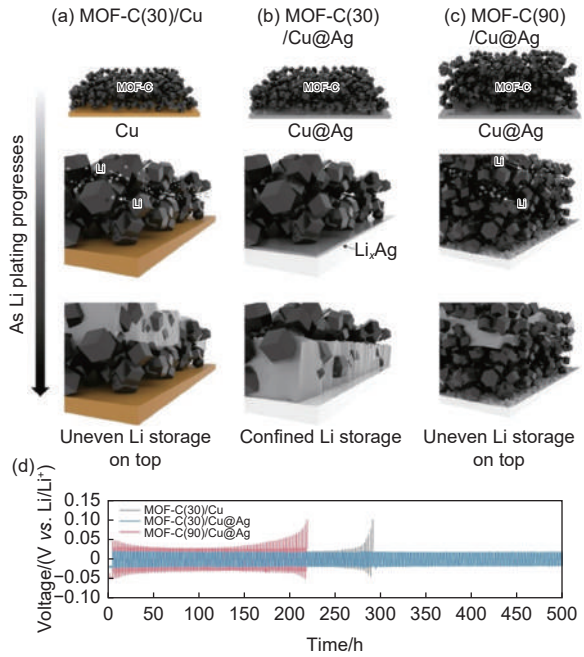

Fig. 3 Schematic diagram of Li plating behaviors of (a) MOF-C(30)/Cu, (b) MOF-C(30)/Cu@Ag, and (c) MOF-C(90)/Cu@Ag[98]. (d) Cycling performance of MOF-C(t)/X//Li pouch cells at 0.4 mAh cm^{-2} and 0.4 mA cm^{-2}. (Reprinted with permission)

holey GO/Li composite anodes[102]. GO/Li composite anode was flexible and had a controllable thickness. The aligned channels in GO host uniformly distributed Li-ion flux and provided short ion transport pathways, which contributed to enhancing rate performance and increased the energy density of the battery (Fig. 4a, b). In a symmetric cell, the holey GO/Li composite anode exhibited a lower overpotential over 400 h than unpunched GO/Li and bare Li anode at 1.3 mA cm^{-2} and 1.3 mAh cm^{-2}. When matched with $LiFePO_4$ (LFP, with a loading of 2.0-2.4 mg cm^{-2}) cathode, the holey GO/Li anode has a capacity of 93.0 mAh g^{-1} at 20 C and stably cycled for more than 600 cycles at 1 C. Likewise, when matched with $LiNi_{0.8}Co_{0.1}Mn_{0.1}O_2$ (NCM811, with a loading of 3.4-4.7 mg cm^{-2}) cathode, the holey GO/Li anode displayed capacity of 117.9 mAh g^{-1} at 10 C and maintained a capacity of more than 150.0 mAh g^{-1} for over 150 cycles at 0.5 C. More notably, in a pouch cell matched with a sulfur/polyacrylonitrile (SPAN) cathode with S loading of 9.8 mg, it displayed an initial capacity of 1 015.0 mAh g^{-1} and capacity retention of 80.0% over 100 cycles.

Low tortuosity of a host has been proven effect-

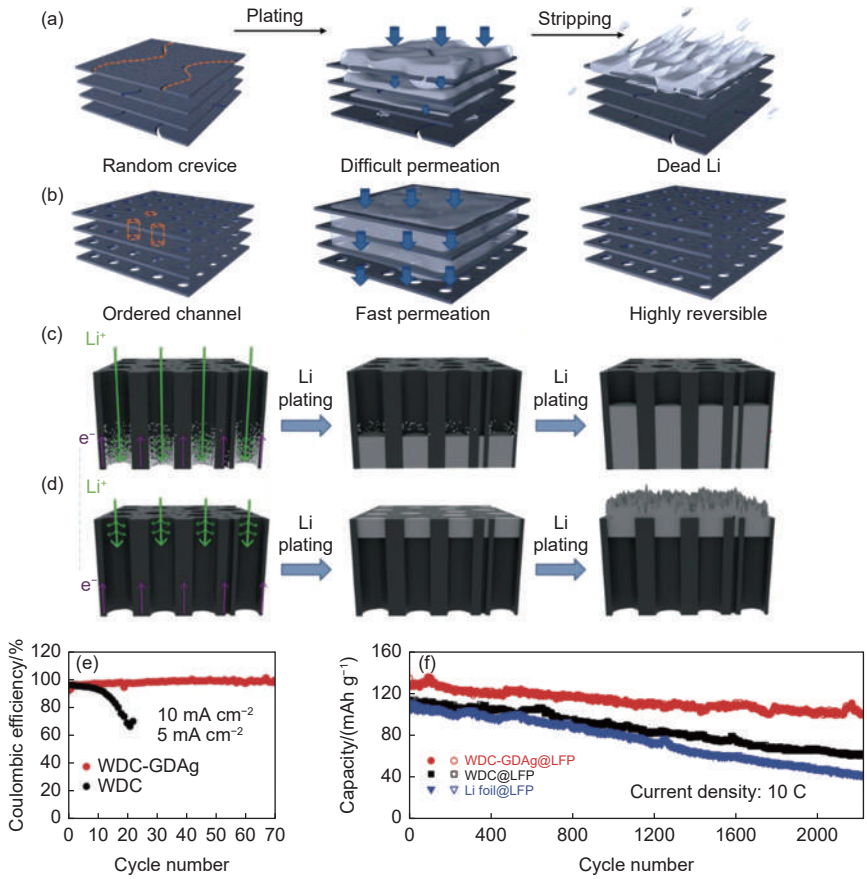

Fig. 4　Schematic diagram of Li plating/stripping of (a) pure GO and (b) holey GO[102]. Schematic diagram of Li plating behaviors of (c) WDC-GDAg and (d) WDC[105]. (e) CE of WDC-GDAg and WDC half cells at 10.0 mA cm^{-2} and 5.0 mAh cm^{-2}. (f) Cycling performance of WDC-GDAg//LFP, WDC//LFP, and Li//LFP at 10 C. (Reprinted with permission)

ive for fast Li ion transport[102–104]. Unfortunately, this structure also results in inhomogeneous local current density, increasing the risk of Li dendrites growth. The gradient distribution of lithiophilic sites in this structure is favorable for achieving synergistic effects. Herein, Zhu et al. introduced the gradient distribution of Ag, ZnO, and Au lithiophilic sites into 3D wood-derived carbon (WDC) host with low tortuosity *via* a capillary-induced gradient deposition[105]. The WDC host decorated with gradient-distributed Ag nanoparticles (WDC-GDAg) could form a high concentration of Li-ion flux at the bottom and a homogeneous electric field distribution at the top, which eventually achieved the bottom-up deposition (Fig. 4c, d). The WDC-GDAg anode maintained the average CE of 98.3% over 70 cycles at 10.0 mA cm^{-2} and 5.0 mAh cm^{-2} (Fig. 4e). When matched with the LFP (with a loading of 4.0 mg cm^{-2}) cathode, the WDC-GDAg//LFP delivered a capacity of 130.0 mAh g^{-1} and a capacity retention of 78.9% over 2 000 cycles at a rate of 10 C (Fig. 4f).

Recently, Cao et al. constructed g-C_3N_4 coated carbon cloth (CC@g-C_3N_4) *via* a thermal polycondensation method, and then infused molten Li into the CC@g-C_3N_4 to obtain CC/Li/Li_3N anode[106]. The g-C_3N_4 reacted with Li to form Li_3N when molten Li infused, and then during the resting process at high temperature, Li_3N gradually diffused and migrated upward to form a Li_3N gradient, which created a gradient lithiophilicity structure in the anode. Owing to the high ionic conductivity and electrochemical stability of Li_3N, the Li_3N-rich artificial SEI layer which was formed by the Li_3N gathered at the top could accelerate the diffusion of Li ions at the interface and prevent continuous side reactions between anode and electrolytes. Density function theory (DFT) results

prove that Li_3N has a low energy barrier of Li ion diffusion. In addition, the rest of Li_3N which was not gathered at the top uniformly disperses in the host, regulating uniform Li deposition (Fig. 5a, b). In symmetric cells, the overpotential of CC/Li/Li_3N electrode was only 80 mV after cycling 1 000 h at 2.0 mA cm^{-2} and 2.0 mAh cm^{-2} (Fig. 5c). When matched with the LFP (with a loading of 2.0 mg cm^{-2}) cathode, CC/Li/Li_3N//LFP cell had an initial discharge capacity of 146.6 mAh g^{-1} at 0.5 C and the capacity retention rate was 93.3% after 150 cycles. Besides, CC/Li/Li_3N//LFP full cell also exhibited improved rate performance than Li//LFP (Fig. 5d). At room temperature, the solid-state battery matching the LFP (with a loading of 2.0 mg cm^{-2}) cathode and garnet (LLZO) electrolytes maintained a capacity of 140.0 mAh g^{-1} after 100 cycles at 0.1 C (Fig. 5e).

Gradient lithiophilic composite anodes could preferentially guide Li deposition inside the bottom of hosts, which plays a positive role in alleviating the volume change of Li and improving the overall space utilization of the host. However, there are still many challenges on the way to practical applications of gradient lithiophilic composite anodes. The preparation of gradient lithiophilic composite anodes requires a complex process and large-scale preparation of gradient lithiophilic host is still a challenge. In addition, it remains unclear whether lithiophilic sites

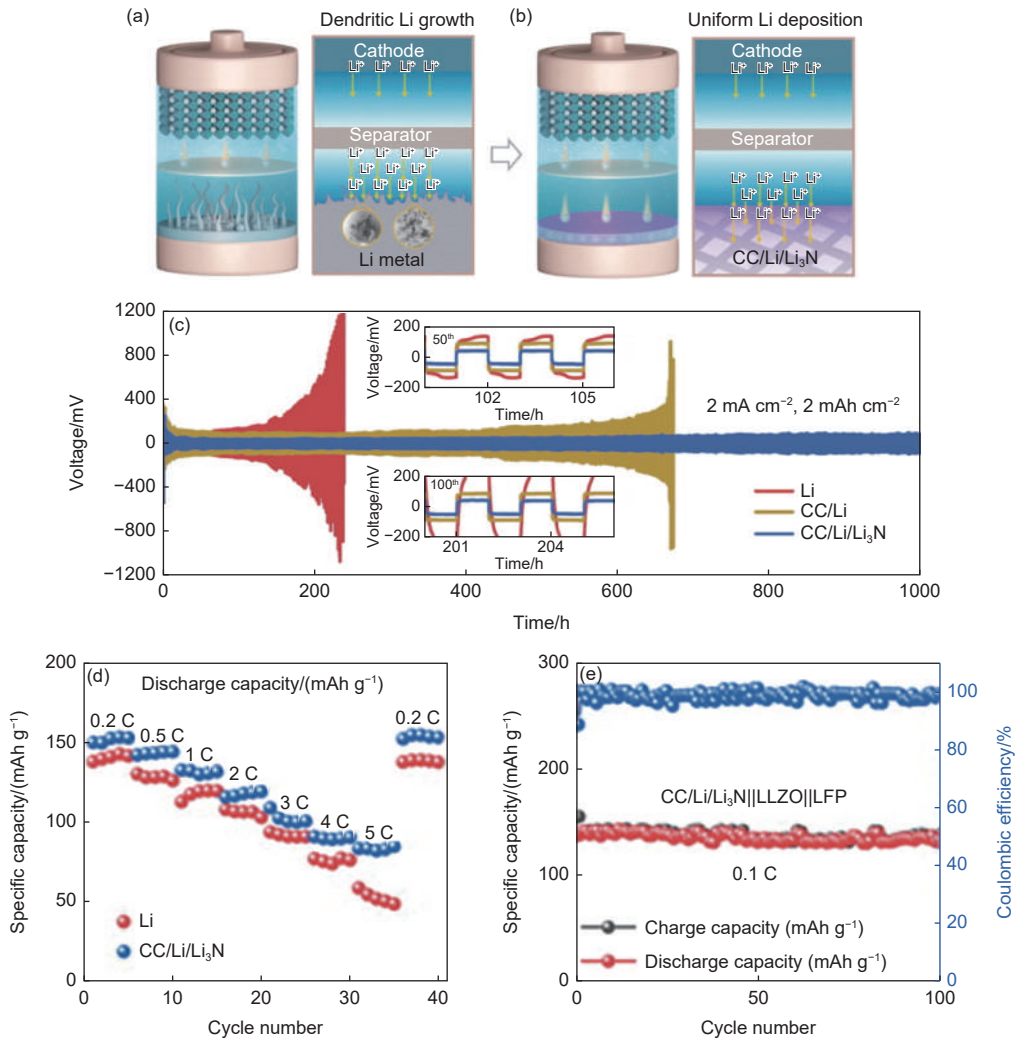

Fig. 5 Schematic diagram of Li plating behaviors of (a) Li//LFP and (b) CC/Li/Li_3N//LFP[106]. (c) Voltage-time curves of bare Li, CC/Li, and CC/Li/Li_3N symmetric cells at 2.0 mA cm^{-2} and 2.0 mAh cm^{-2}. (d) Rate performance of CC/Li/Li_3N//LFP and bare Li//LFP full cell. (e) Cycling performance of CC/Li/Li_3N//LLZO//LFP at 0.1 C for 100 cycles. (Reprinted with permission)

would fall off or the structure of lithiophilic sites change during the repeated Li plating/stripping.

2.2 Gradient conductivity

Similar to gradient lithiophilicity, gradient conductivity is constructed by using the material with high conductivity at the bottom of the host and the material with low conductivity or electrical insulation at the top of the host, so that the conductivity decreases from bottom to top continuously. Gradient conductive composite Li anodes could control the distribution of electric field and induce Li to preferentially deposit on the host material with high conductivity.

Initial studies of gradient conductivity hosts focus on combining metal with polymer materials. Hong et al. constructed a conductivity gradient host (CG) composed of conductive copper nanowires (CuNWs) and insulating cellulose nanofibers (CNFs) *via* a vacuum-assisted infiltration process[107]. The bottom layer was CuNWs with high conductivity, the middle layer was a mixture of CuNWs and CNFs with low conductivity, and the top insulating layer was a mixture of CNFs and SiO_2 nanoparticles. SiO_2 nanoparticles in the top area of CG could exhibited superior wettability with electrolytes, increasing Li-ion flux on polar groups of the CNFs (Fig. 6a-c). Experiments and COMSOL multiphysics simulation revealed that when the thickness of the top insulating layer was 1 μm and the difference in conductivity between the middle and bottom layer was 6 kS cm^{-1}, Li preferentially deposited at the bottom of the CG host. In symmetric cells, CG electrode maintained low voltage hysteresis for about 250 cycles at 1.0 mA cm^{-2} and 1.0 mAh cm^{-2}. Besides, CG was stable for 100 cycles when the current density increased to 5.0 mA cm^{-2}. When matched with a NCM811 (with a loading of ~ 1.1 mAh cm^{-2}) cathode, the capacity retention of the full cell (N/P ratio of 3.6) was more than 90.0% after 100 cycles at 1 C.

Li et al. prepared nickel (Ni) metal on one side of melamine sponge to form a conductive-dielectric gradient host (CDG-sponge) by magnetron sputtering[108]. For comparison, a fully conductive host

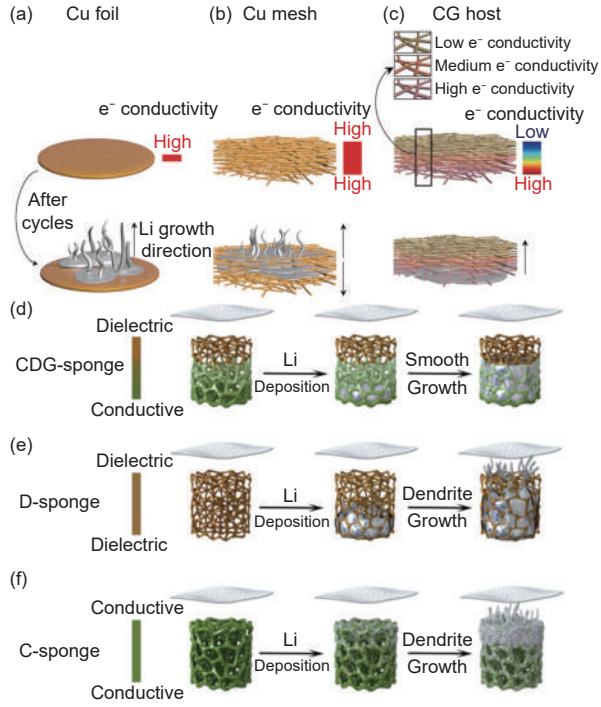

Fig. 6　Schematic diagram of Li plating behaviors of (a) Cu foil, (b) Cu mesh, and (c) CG host[107]. Schematic diagram of Li plating behaviors of (d) CDG-sponge: bottom deposition without dendrite formation. (e) D-sponge: bottom deposition with dendrite formation. (f) C-sponge: top deposition with dendrite formation near the separator[108]. (Reprinted with permission)

(C-sponge) and a dielectric host (D-sponge) were also fabricated. The thickness of the conductive Ni coating layer of CDG-sponge attenuated upward, and the top area was bare melamine, forming a conductivity gradient to achieve bottom-up deposition and top-down stripping pattern of Li (Fig. 6d-f). Melamine with polar functional groups (*e.g.*, amine group) could adsorb Li ions and homogenize Li-ion flux. Before assembling symmetric cells, 3.0 mAh cm^{-2} of Li was first deposited on the CDG-sponge (Li@CDG-sponge). At 1.0 mA cm^{-2} and 1.0 mAh cm^{-2}, Li//Li@CDG-sponge cell showed a low polarization voltage (< 20 mV) and a long lifespan (780 h). Matched with LFP (with a loading of 4.0 mg cm^{-2}) cathode, Li@CDG-sponge//LFP cell maintained a capacity of 127.3 mAh g^{-1} after 400 cycles at 1 C with a capacity retention of 87.6%.

Inspired by these studies above, research on carbon-based hosts with gradient conductivity was initiated. Zou et al. stacked polyacrylonitrile (PAN) membranes and carbon nanofiber (CNF) membranes in sequence to form a periodic PAN/CNF host[109]. PAN

membranes acted as dielectric layers to periodically separate the conductive layers (*i.e.*, CNF membranes), blocking the electronic transport pathways from the bottom conductive layer to the upper conductive layer. Only when the plated Li metal connected the 2 conductive layers could electronic pathways be formed. More importantly, if Li dendrites were formed and grown to contact with the upper conductive layer, the electric field could be re-homogenized, and the local current density of the dendrites would decrease significantly, presenting a self-correction effect (Fig. 7a). Consequently, Li could be deposited smoothly at high current density and high cycling capacity, following a bottom-up pattern (Fig. 7b). 10.0 mAh cm^{-2} of Li metal plating in periodic PAN/CNF host was denoted as Li@PAN/CNF. At 5.0 mA cm^{-2} and 5.0 mAh cm^{-2}, Li@PAN/CNF//Li@PAN/CNF symmetric cell delivered a stable voltage hysteresis for over 800 cycles. When matched with the $LiNi_{0.6}Co_{0.2}Mn_{0.2}O_2$ (NCM622, with a loading of ~ 12.0 mg cm^{-2}) cathode, Li@PAN/CNF//NCM622 cell displayed an initial capacity of 153.0 mAh g^{-1} at 1 C and the capacity retention of 87.0% after 100 cycles. Likewise, matched with the NCM811 (with a loading of ~ 20.0 mg cm^{-2}) cathode, Li@PAN/CNF//NCM811 full cell delivered an initial capacity of 3.5 mAh cm^{-1} at 1 C and maintained 70.0% capacity after 100 cycles.

Sun et al. synthesized a gradient topological host consisting of SiC whiskers and carbon cloth (SiC/CC) *via* a gas-solid reaction of gaseous SiO with porous CC[110]. During the reaction, the gas concentration of SiO increased with the height of the CC host and concentrated at the top surface, forming a CC host with gradient-decorated SiC whiskers. A gradient conductivity structure was derived from the conductivity difference between semiconductive SiC and conductive carbon fibers. The topological structure in SiC/CC host could not only ensure contacts with the deposited Li reducting inactive Li but also effectively regulate the distribution of electric field and Li-ion flux, which was conducive to a uniform deposition of Li (Fig. 7c). In addition, Li would react with C or Si of the SiC/CC host to from Li-Si and Li-C alloys[111], which could reduce Li nucleation barriers. In half cells, SiC/CC electrode remained at a high CE (> 95.0% of the initial CE) after 100 cycles at 1.0 mA cm^{-2} and 1.0 mAh cm^{-2} and kept stable after 50 cycles at 5.0 mA cm^{-2} and 3.0 mAh cm^{-2}. Li@SiC/CC (with an average mass loading of 5.0 mAh cm^{-2}) symmetric cell maintained a low overpotential (< 20 mV) for over 1 000 h at 1.0 mA cm^{-2} and 1.0 mAh cm^{-2}, and showed a lifespan of over 320 h at 5.0 mA cm^{-2} and 5.0 mAh cm^{-2}. When Li@SiC/CC (3.0 mAh cm^{-2}) anode matched with the LFP (with a loading of 4.5 mg cm^{-2}) cathode, Li@SiC/CC//LFP cell (N/P ratio of 4.4) showed a capacity of 120.0 mAh g^{-1} after 120 cycles with the capacity retention of 80.0% at 0.5 C (Fig. 7d).

Modification of the top area of the carbon-based gradient host is conducive to the formation of stable SEI and maintaining the gradient conductivity structure. Zhou et al. combined a dielectric top layer with the decorated $LiNO_3$ particles and CNF layers with

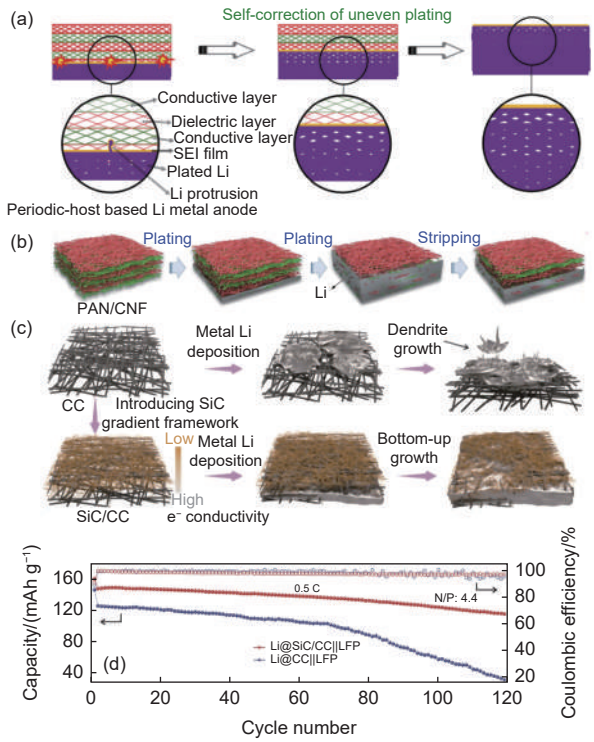

Fig. 7 (a) Schematic diagram of Li metal evolution in periodic-host based Li metal anode showing a "self-correction" behavior, and (b) schematic diagram of Li plating/stripping of the periodic PAN/CNF host[109]. (c) Schematic diagram of Li plating behaviors of CC and SiC/CC host, and (d) cycling performance of the Li@Cu//LFP and Li@SiC/CC//LFP full cell at 0.5 C[110]. (Reprinted with permission)

gradient conductivity to form a $LiNO_3$-modified conductivity gradient host (LNO-CGH)[112]. LNO-CGH consisted of 4 layers. Namely, the lower 3 layers were CNF layers with different concentrations of CNTs. Among them, the bottom layer corresponded to the spinning solution with 10.0% mass ratio of CNTs and PAN (10CCNF), and the upper 2 layers corresponded to the spinning solution with 5.0% and 0% mass ratio of CNTs and PAN (5CCNF and CNF), forming a conductivity gradient. The top layer was a dielectric PAN film with $LiNO_3$ particles (LNO-PAN), which had the lowest conductivity and could continuously release a limited amount of $LiNO_3$ into the electrolytes during cycles, promoting the formation of a robust SEI and improving the thermodynamic stability of anode (Fig. 8a-c). In half cells, the average CE of LNO-CGH was 97.4% over 200 cycles at 1.0 mA cm^{-2} and 2.0 mAh cm^{-2}. When the current density and cycling capacity increased to 2.0 mA cm^{-2} and 5.0 mAh cm^{-2}, the LNO-CGH electrode maintained an average CE of 97.3% over 60 cycles. Before assembling the full cell, 5.0 mAh cm^{-2} of Li was deposited on the LNO-CGH host (LNO-CGH@Li) as an anode. When matched with the $LiNi_{1/3}Co_{1/3}Mn_{1/3}O_2$ (NCM111, with a loading of 9.5 mg cm^{-2}) cathode, LNO-CGH@Li//NCM111 cell (N/P ratio of 4.0) displayed the capacity retention of 74.9% after 120 cycles at 1 C. Similarly, matched with the NCM811 (with a loading of 11 mg cm^{-2}) cathode, LNO-CGH@Li//NCM811 cell (N/P ratio of 2.3) maintained 72.9% capacity retention after 60 cycles at 1 C (Fig. 8d). A flexible quasi-solid Li metal battery composed of LNO-CGH@Li (5.0 mAh cm^{-2}) anode, flexible NCM811@PCNF1000 (with a loading of 5.5 mg cm^{-2}) cathode, and P(VDF-HFP)-based gel polymer separator showed a capacity of 191.4 mAh g^{-1} at 1 C and capacity retention of 78.2% after 100 cycles (Fig. 8e).

Gradient conductive composite Li anodes could guide Li deposition following a bottom-up pattern by reducing the local current density at the top of a host. Nevertheless, due to the high conductivity of Li metal, the electric field would change as Li deposits continuously. Thus, gradient conductive composite Li anodes may not be able to exhibit advantages in the repeated

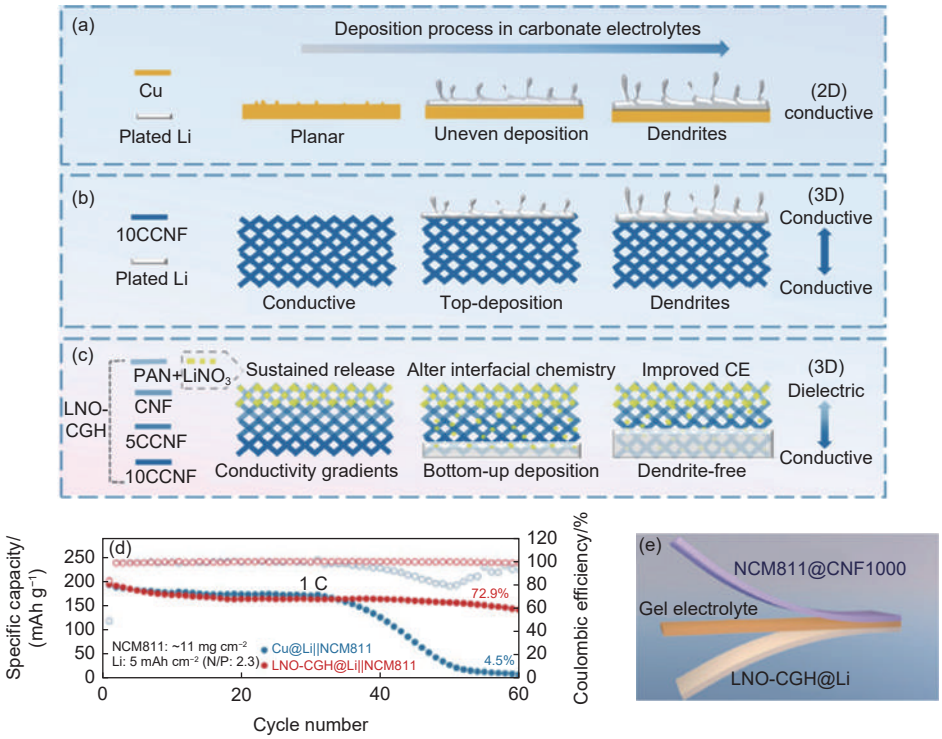

Fig. 8　Schematic diagram of Li plating behaviors of (a) Cu foil, (b) 10CCNF and (c) LNO-CGH[112]. (d) Cycling performance of Cu@Li//NCM811 and LNO-CGH@Li//NCM811 full cell at 1 C. (e) Schematic of flexible quasi-solid Li metal battery (LNO-CGH@Li//Gel electrolytes//NCM811@PCNF1000). (Reprinted with permission)

Li stripping/plating process.

2.3 Dual gradient

In order to combine the advantages of gradient lithiophilicity and conductivity, composite Li anodes with dual gradient are proposed, in which lithiophilic sites on the conductive materials are located at the bottom of the host and the lithiophobic materials with low conductivity are placed at the top of the host. The dual gradient could regulate ion and electron conducting pathways simultaneously and synergistically guide homogeneous Li deposition from bottom to top.

Pu et al. constructed a deposition-regulating scaffold (DRS) with a dual gradient[113]. They first prepared a porous bare nickel scaffold (BNS) *via* templated electrodeposition and selective etching. Then, the top of BNS was coated with alumina (Al_2O_3) for electrical passivation and the bottom area was activated by an Aurum (Au) layer to reduce Li nucleation barrier. The Al_2O_3 coating at the top area of DRS reduced local conductivity, creating a conductivity gradient with conductive metal Ni/Au at the bottom of the host. Likewise, lithiophilic Au at the bottom of DRS showed almost zero nucleation barrier, while high-barrier Al_2O_3 coating was at the top area, together forming a lithiophilicity gradient. Under the synergistic regulation of gradient conductivity and lithiophilicity, Li deposited following a bottom-up pattern in the DRS (Fig. 9a-b). Under different test conditions (*i.e.*, current density and cycling capacity), DRS electrode presented higher CE and a longer lifespan than BNS and Cu foil. It is noteworthy that Li was preferentially deposited at the bottom of DRS even at low-temperature conditions (5 and −15 °C), and the DRS cell could keep 50 cycles with no voltage fluctu-

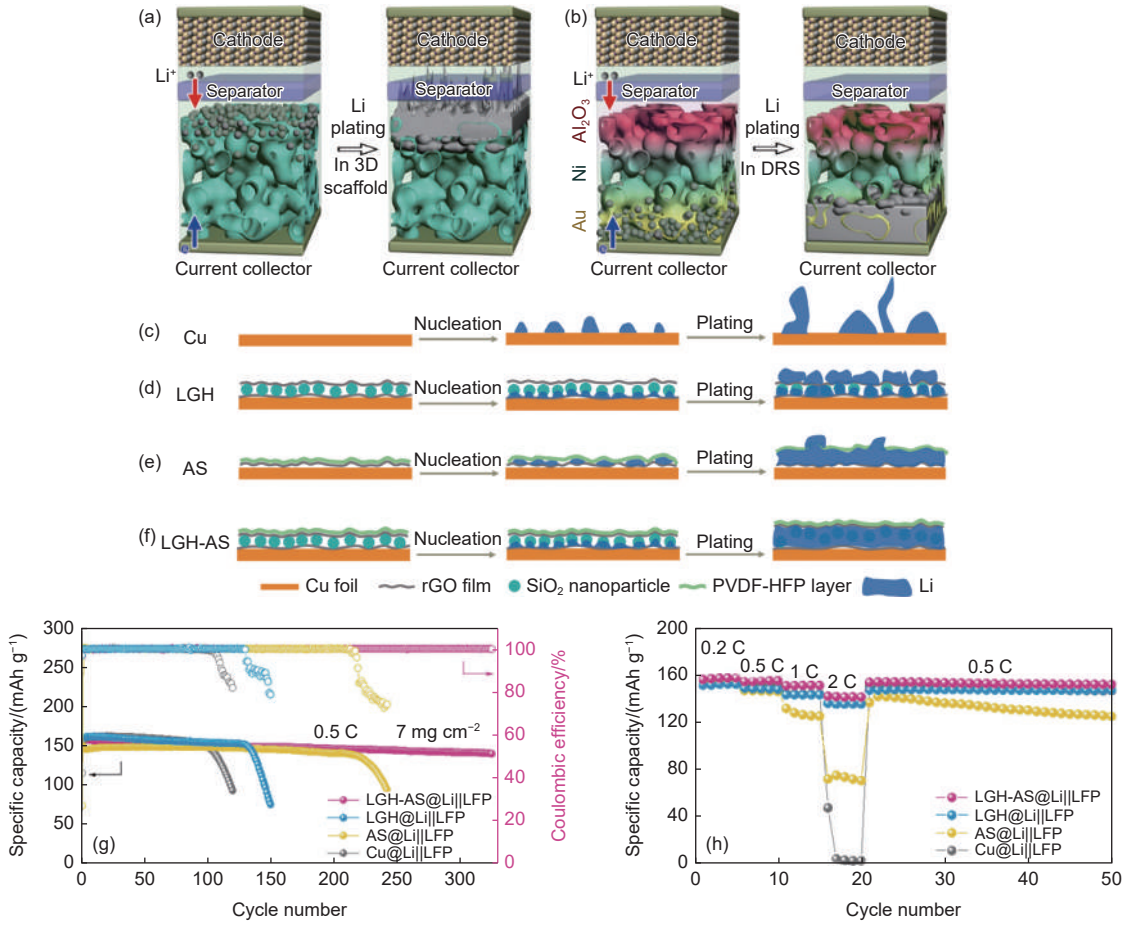

Fig. 9 Schematic diagram of Li plating behaviors of (a) BNS following the top-growth mode and (b) DRS following the bottom–up mode[113]. Schematic diagram of Li plating behaviors of (c) Cu with uneven nucleation and dendrite. (d) LGH with inter deposition and low pore utilization. (e) AS with first deposition between rGO and PVDF-HFP layer and then on AS because of the fragile polymer coating, and (f) LGH-AS with Li deposition from bottom to top in SiO_2-embedded interlayer[114]. (g) Cycling performance of full cells at 0.5 C. (h) Rate performance of full cells from 0.2 to 2.0 C. (Reprinted with permission)

ation at −15 °C.

Cai et al. designed a sandwich-like gradient host with an artificial SEI (LGH-AS), composed of rGO, SiO_2, rGO and poly(vinylidene fluoride-co-hexafluoropropylene) (PVDF-HFP) in a bottom-up sequence (Fig. 9c, f)[114]. Simultaneously, LGH and AS were fabricated. LGH consisted of two layers of rGO and SiO_2 interlayer (Fig. 9d), while AS was composed of bottom rGO and PVDF-HFP (Fig. 9e). In LGH-AS, the bottom rGO layer was tightly anchored to Cu foil and conducted electrons from the foil. SiO_2 interlayer provided lithiophilic sites and simultaneously prevented the bottom and upper rGO layers from contacting and forming electronic pathways. The upper rGO layer prevented SiO_2 from falling off and endowed mechanical strength to inhibit Li dendrites. The PVDF-HFP layer kept the whole electrode surface insulated and guided Li plating in SiO_2 interlayer. SiO_2 and Li would react to form an irreversible Li_2O phase on the particle surface, which could uniform Li-ion flux[115]. The average CE of LGH-AS electrode was 98.1% throughout 275 cycles at 0.5 mA cm^{-2} and 0.5 mAh cm^{-2}. When cycling capacity increased to 5.0 mAh cm^{-2}, LGH-AS exhibited an average CE of 99.1% for 60 cycles. 4.0 mAh cm^{-2} of Li was pre-deposited on LGH-AS (LGH-AS@Li) as an anode, matching with the LFP (with a loading of 7 mg cm^{-2}) cathode to assemble a full cell, which exhibited capacity retention of 90.2% after 300 cycles at 0.5 C and a better rate performance than the other 3 cells from 0.2 C to 2 C (Fig. 9g-h).

Zeolite imidazolate framework (ZIF) is a class of MOFs with excellent chemical and thermal stability[116]. ZIF-8 is a porous material consisting of zinc ions (Zn^{2+}) and imidazolium ligands. Shi et al. prepared ZIF-8-derived gradient interfacial layer (ZGIL) *via* a two-step lamination method, with ZIF-8 and polyvinylidene fluoride (PVDF) at the top layer and carbonized ZIF-8 (C-ZIF-8) and CNT dispersion at the bottom layer (Fig. 10a)[117]. C-ZIF-8 at the bottom layer of ZGIL provided high Li-ion and electron conductivity, and the Zn clusters or single atoms in it exhibited excellent lithiophilicity. ZIF-8 as a surface

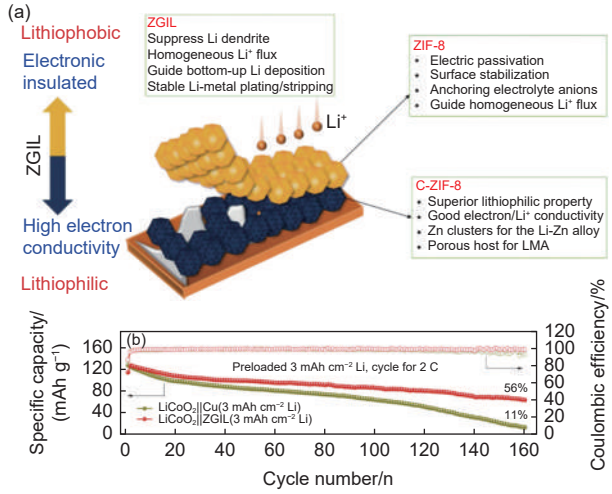

Fig. 10　(a) Schematic diagram of ZGIL coated Cu foil. (b) Cycling performance of $LiCoO_2$//ZGIL and $LiCoO_2$//Cu full cell at 2 C[117]. (Reprinted with permission)

electric passivation layer could suppress the top deposition of Li. Moreover, the high Li-ion conductivity of ZIF-8 could not only enhance the rapid diffusion of Li ions and homogenize Li-ion flux, but also release a large amount of Li ions by anchoring anions in electrolytes, such as bis trifluoromethyl sulfonic acid amide ions and hexafluorophosphate ions ($TFSI^-$ and PF_6^-). The average CE of ZGIL-Cu electrode was 97.6% over 300 cycles at 1.0 mA cm^{-2} and 1.0 mAh cm^{-2}. The ZGIL-Li modified symmetric cell cycled for over 700 h at 1.0 mA cm^{-2} and 1.0 mAh cm^{-2}, and it exhibited better rate performance than bare Li and C-ZIF-8-Li. In full cells, the ZGIL-modified Cu foil with Li (3.0 mAh cm^{-2}) was used as the anode. While matching with the $LiCoO_2$ (with a loading of 4.6 mg cm^{-2}) cathode, $LiCoO_2$//ZGIL cell (N/P ratio of 6.0) remained 56.0% capacity retention after 160 cycles at 2 C (Fig. 10b).

The combination of 3D porous hosts and gradient structures could indeed uniform Li deposition, following a bottom-up deposition pattern. Nevertheless, this synergistic effect is generally achieved by adopting a thick host at the expense of volume energy density[118–119]. Yu et al. designed a thin (6-8 μm) composite host, namely a gradient Ag decorated graphene/holey graphene film (G-HGA), which was composed of Ag decorated GO (AgGO), Ag decorated GO

mixed with holey GO (AgGO-hGO), and hGO hydrogels in a bottom-up sequence[120]. The concentration of Ag nanoparticles (AgNPs) decreased from bottom to up, constituting lithiophilicity and conductivity gradient simultaneously. hGO provided sufficient mechanical strength, and the hole defects of hGO shortened Li ion transport pathways and facilitated the fast transport of Li ions. The average CE of Li//G-HGA cell was 98.8% for 350 cycles at 1.0 mA cm^{-2} and 1.0 mAh cm^{-2}. When the cycling capacity was increased to 2.0 mAh cm^{-2}, G-HGA electrode maintained high stability over 400 cycles. At 1.0 mA cm^{-2} and 1.0 mAh cm^{-2}, G-HGA@Li//G-HGA@Li (with 4.0 mAh cm^{-2} deposited Li) symmetric cell delivered a cycling lifespan for over 600 h. When G-HGA@Li (3.0 mAh cm^{-2}) anode was matched with LFP (with a loading of 2.7 mAh cm^{-2}) cathode, G-HGA@Li//LFP cell (N/P ratio of 1.1) showed a capacity of 159.0 mAh g^{-1} at 0.2 C, and capacity retention of 99.6% after 175 cycles at 0.5 C.

Dual gradient composite Li anodes could steer Li ions to accumulate at the bottom of the host, and regulate homogeneous stripping/plating behavior of Li, achieving the synergistic effect of guiding Li bottom-up deposition pattern. However, most designs of dual gradient composite Li anodes consist of many layers with different properties, which form thick hosts at the expense of the energy density of Li metal batteries.

3 Outlooks

Gradient composite Li anodes could guide the bottom-up deposition pattern of Li and improve the space utilization efficiency of hosts. Since Li stripping/plating process is regulated by the electronic and ionic pathways, the gradient hosts could be divided into gradient lithiophilicity, gradient conductivity and dual gradient. Various strategies have been proposed to prepare carbon-based gradient composite Li anodes (Table 1). However, the veritably working mechanism and effectiveness under practical conditions, especially in pouch cells, of gradient composite Li anodes are still controversial. In order to further promote the development of gradient composite Li anodes, the following aspects are suggested:

(1) Effectiveness under practical conditions. Practical conditions are necessary for achieving high specific energy of Li metal batteries. However, most research employs coin cells under mild conditions (*i.e.*, thick Li and flooded electrolytes). There is a large gap between the performance under mild and practical conditions for Li metal batteries[121–122]. To explore the practical applications of gradient composite Li anodes, practical conditions such as high-loading cathode (> 4.0 mAh cm^{-2}), limited Li (< 10.0 mAh cm^{-2}), and lean electrolytes (< 3.0 g Ah^{-1}) and pouch cell measurements should be considered.

(2) Optimization of host structure parameters. The increase of pore size from bottom to top could accelerate the transport of Li ions[123–124]. The pore gradient could be combined with lithiophilicity gradient and conductivity gradient to synergistically regulate Li stripping/plating process. Owing to the layers with different properties, the gradient hosts are usually thick, which reduces the energy density of batteries. To obtain a high specific energy battery, the thickness of gradient composite Li anodes should be controlled.

(3) Failure analysis of gradient design. For the lithiophilic composite Li anodes, inactive Li could cover lithiophilic sites and block Li ion transport pathways towards lithiophilic sites during cycles, inducing hosts to lose their gradient lithiophilicity[125]. Similarly, electric field could vary due to Li deposition with high conductivity. Therefore, it is necessary to investigate the failure mechanism of gradient design and corresponding strategies which could prolong the lifespan of gradient composite Li anodes and enhance the cycling stability of Li metal batteries.

(4) Exploring Li plating/stripping mechanism in gradient composite Li anodes. Understanding the Li plating/stripping mechanism, especially during repeated cycles, in gradient composite Li anodes by advanced characterization tools or theoretical simulations could provide rational guidance for further design of gradient composite Li anodes. Ingenious experimental design is also required to decouple the ef-

Table 1　Comparison of full cell and pouch cell performance of carbon-based gradient composite anodes

Type	Sample	Coin cell	Pouch cell	Electrolyte	Ref.
Gradient lithiophilicity	GZCNT	GZCNT-coated Li//S ($2.5\ mg\ cm^{-2}$) 0.2 C, 200 cycles	Symmetric GZCNT-coated Li pouch cell $1.0\ mA\ cm^{-2}$, $1.0\ mAh\ cm^{-2}$, 200 cycles	0.6 mol L^{-1} LiTFSI in DOL/DME (1 : 1, *w*/*w*) with 0.4 mol L^{-1} $LiNO_3$	[96]
	GSCP	GSCP@Li (5.0 mAh)//LTO (~ $1.2\ mg\ cm^{-2}$) 10 C, 5000 cycles	N.A.	1.0 mol L^{-1} LiTFSI in DOL/DME (1 : 1, *v*/*v*) with 1 wt% $LiNO_3$	[97]
	MOF-C(*t*)/X	N.A.	MOF-C(*t*)/X//Li $0.5\ mA\ cm^{-2}$, $1\ mAh\ cm^{-2}$, nucleation overpotential of MOF-C(30)/Cu@Ag was 6 mV	1.0 mol L^{-1} LiTFSI in DOL/DME (1 : 1, *v*/*v*) with 1 wt% $LiNO_3$	[98]
	Holey GO/Li	holey GO/Li//LFP ($2.0\text{-}2.4\ mg\ cm^{-2}$) 1 C, 500 cycles holey GO/Li//NCM811 ($3.4\text{-}4.7\ mg\ cm^{-2}$) 0.5 C, 150 cycles	Holey GO/Li//SPAN (S: 9.75 mg) 0.2 C, 100 cycles	1.0 mol L^{-1} $LiPF_6$ in EC/DEC (1 : 1, *v*/*v*) with 1% VC and 10% FEC	[102]
	WDC-GDAg	WDC-GDAg//LFP ($4\ mg\ cm^{-2}$) 10 C, 2000 cycles	N.A.	1.0 mol L^{-1} LiTFSI in DOL/Dimethoxymethane (1 : 1, *v*/*v*) with 1 wt% $LiNO_3$	[105]
	CC/Li/Li_3N	CC/Li/Li_3N//LFP ($2.0\ mg\ cm^{-2}$) 0.5 C, 150 cycles	Solid-state battery at room temperature: CC/Li/Li_3N//LLZO//LFP ($2.0\ mg\ cm^{-2}$) 0.1 C, 100 cycles	1.0 mol L^{-1} $LiPF_6$ in EC/EMC (3 : 7, *v*/*v*)	[106]
Gradient conductivity	CG	CG@Li//NCM811 (~ $1.1\ mAh\ cm^{-2}$, N/P ratio of 3.6) 1 C, 100 cycles	N.A.	1.0 mol L^{-1} $LiPF_6$ in EC/DEC (1 : 1, *v*/*v*) with 1 wt% VC	[107]
	CDG-sponge	Li@CDG-sponge ($3.0\ mAh\ cm^{-2}$)//LFP ($4.0\ mg\ cm^{-2}$) 1 C, 400 cycles	N.A.	1.0 mol L^{-1} LiTFSI in DOL/DME (1 : 1, *v*/*v*) with 2 wt% $LiNO_3$	[108]
	PAN/CNF	Li@PAN/CNF//NCM811 (~ $20.0\ mg\ cm^{-2}$) 1 C, 100 cycles	N.A.	1.0 mol L^{-1} $LiPF_6$ in EC/EMC/DMC (1 : 1 : 1, *v*/*v*/*v*)	[109]
	SiC/CC	Li@SiC/CC ($3.0\ mAh\ cm^{-2}$)// LFP ($4.5\ mg\ cm^{-2}$) 0.5 C, 120 cycles	N.A.	1.0 mol L^{-1} LiTFSI in DOL/DME (1 : 1, *v*/*v*) with 2 wt% $LiNO_3$	[110]
	LNO-CGH	LNO-CGH@Li ($5.0\ mAh\ cm^{-2}$)// NCM811 ($11\ mg\ cm^{-2}$) 1 C, 60 cycles	Flexible quasi-solid Li metal battery: LNO-CGH@Li ($5.0\ mAh\ cm^{-2}$)// Gel electrolyte// NCM811@PCNF1000 ($5.5\ mg\ cm^{-2}$) 1 C, 100 cycles	1.0 mol L^{-1} $LiPF_6$ in EC/DEC (1 : 1, *w*/*w*) with 5% FEC	[112]
Dual gradient	LGH-AS	LGH-AS@Li ($4.0\ mAh\ cm^{-2}$)// LFP ($7.0\ mg\ cm^{-2}$) 0.5 C, 300 cycles	N.A.	1.0 mol L^{-1} LiTFSI in DOL/DME (1 : 1, *v*/*v*) with 1% $LiNO_3$	[114]
	ZGIL	ZGIL ($3.0\ mAh\ cm^{-2}$)// $LiCoO_2$ ($4.6\ mg\ cm^{-2}$) 2 C, 160 cycles	N.A.	1.0 mol L^{-1} $LiPF_6$ in EC/DEC (1 : 1, *w*/*w*) with 30% FEC	[117]
	G-HGA	G-HGA@Li ($3.0\ mAh\ cm^{-2}$)// LFP ($2.7\ mAh\ cm^{-2}$) 0.5 C, 175 cycles	N.A.	1.0 mol L^{-1} LiTFSI in DOL/DME (1 : 1, *v*/*v*) with 2% $LiNO_3$	[120]

fect of host properties on the behavior of Li plating/stripping because there are intersectant effects between different properties.

(5) Large-scale preparations of gradient composite Li anodes. Nowadays, the preparations of gradient composite Li anodes are generally complex. Thus, the consistency during large-scale preparations should be carefully evaluated, and simple technologies are pursued. In addition, when it comes to practical applications, the cost should be considered, which should be taken into consideration during the design of gradient composite Li anodes.

In summary, gradient composite Li anodes have the potential to regulate the bottom-up deposition of Li and achieve a uniform Li deposition morphology, which is essential for the development of Li metal batteries. However, there are still practical challenges that need to be addressed in order to implement gradient composite Li anodes in practical applications despite their potential benefits. Therefore, it is important to gain a deep understanding of the regulation and failure mechanisms of these anodes, and to design a

host material that considers various aspects to find the optimal solution. By doing so, we could pave the way for the practical applications of high-energy-density Li metal batteries based on composite Li anodes.

Acknowledgements

This work was supported by National Key Research and Development Program (2021YFB2400300), the Beijing Natural Science Foundation (JQ20004), the National Natural Science Foundation of China (22209010 and 22109007), the China Postdoctoral Science Foundation (2021M700404), the Beijing Institute of Technology Research Fund Program for Young Scholars.

References

[1] Zhang X Q, Li T, Li B Q, et al. A sustainable solid electrolyte interphase for high-energy-density lithium metal batteries underpractical conditions[J]. Angewandte Chemie International Edition, 2020, 59(8): 3252-3257.

[2] Zhou M Y, Ding X Q, Ding J F, et al. Quantifying the apparent electron transfer number of electrolyte decomposition reactions in anode-free batteries[J]. Joule, 2022, 6(9): 2122-2137.

[3] Wang Y Y, Zhang X Q, Zhou M Y, et al. Mechanism, quantitative characterization, and inhibition of corrosion in lithium batteries[J]. Nano Research Energy, 2023, 2: e9120046.

[4] Schmuch R, Wagner R, Hörpel G, et al. Performance and cost of materials for lithium-based rechargeable automotive batteries[J]. Nature Energy, 2018, 3(4): 267-278.

[5] Yuan H D, Ding X F, Liu T F, et al. A review of concepts and contributions in lithium metal anode development[J]. Materials Today, 2022, 53: 173-196.

[6] Sun W, Li Q M, Xiao P, et al. Effect of a compressed separator on the electrochemical performance of Li-ion battery[J]. Journal of Power Sources, 2023, 563: 232835.

[7] Bi C X, Hou L P, Li Z, et al. Protecting lithium metal anodes in lithium–sulfur batteries: A review[J]. Energy Material Advances, 2023, 4: 0010.

[8] Yuan S Y, Kong T Y, Zhang Y Y, et al. Advanced electrolyte design for high-energy-density Li-metal batteries under practical conditions[J]. Angewandte Chemie International Edition, 2021, 60(49): 25624-25638.

[9] Shen X, Zhang X Q, Ding F, et al. Advanced electrode materials in lithium batteries: Retrospect and prospect[J]. Energy Material Advances, 2021, 2021: 1205324.

[10] Fu W B, Kim D, Wang F J, et al. Stabilizing cathodes and interphases for next-generation Li-ion batteries[J]. Journal of Power Sources, 2023, 561: 232738.

[11] Liu H, Cheng X B, Chong Y, et al. Advanced electrode processing of lithium ion batteries: A review of powder technology in battery fabrication[J]. Particuology, 2021, 57: 56-71.

[12] Cheng X B, Liu H, Yuan H, et al. A perspective on sustainable energy materials for lithium batteries[J]. SusMat, 2021, 1(1): 38-50.

[13] Zhang X, Yang Y A, Zhou Z. Towards practical lithium-metal anodes[J]. Chemical Society Reviews, 2020, 49(10): 3040-3071.

[14] Sun S Y, Yao N, Jin C B, et al. The crucial role of electrode potential of a working anode in dictating the structural evolution of solid electrolyte interphase[J]. Angewandte Chemie International Edition, 2022, 61(42): e202208743.

[15] Shi P, Hou L P, Jin C B, et al. A successive conversion-deintercalation delithiation mechanism for practical composite lithium anodes[J]. Journal of the American Chemical Society, 2022, 144(1): 212-218.

[16] Zheng H F, Zhang Q F, Chen Q L, et al. 3D lithiophilic–lithiophobic–lithiophilic dual-gradient porous skeleton for highly stable lithium metal anode[J]. Journal of Materials Chemistry A, 2020, 8(1): 313-322.

[17] Nanda S, Gupta A, Manthiram A. Anode-free full cells: A pathway to high-energy density lithium-metal batteries[J]. Advanced Energy Materials, 2021, 11(2): 2000804.

[18] Jin C B, Shi P, Zhang X Q, et al. Advances in carbon materials for stable lithium metal batteries[J]. New Carbon Materials, 2022, 37(1): 1-24.

[19] Zhang H Y, Ju S L, Xia G L, et al. Identifying the positive role of lithium hydride in stabilizing Li metal anodes[J]. Science Advances, 2022, 8(3): eabl8245.

[20] Liu H, Cheng X B, Yan C, et al. A perspective on energy chemistry of low-temperature lithium metal batteries[J]. iEnergy, 2022, 1(1): 72-81.

[21] Jiang Z P, Li A, Meng C Y, et al. Strategies and challenges of carbon materials in the practical applications of lithium metal anode: a review[J]. Physical Chemistry Chemical Physics, 2022, 24(43): 26356-26370.

[22] Bi C X, Zhao M, Hou L P, et al. Anode material options toward 500 Wh kg^{-1} lithium-sulfur batteries[J]. Advanced Science, 2022, 9(2): 2103910.

[23] Vincent C A. Lithium batteries: A 50-year perspective, 1959–2009[J]. Solid State Ionics, 2000, 134: 159-167.

[24] Zhang Y F, Wu S C, Yang Q H. Revisiting lithium metal anodes from a dynamic and realistic perspective[J]. EnergyChem, 2021, 3(5): 100063.

[25] Pu J, Li J C, Shen Z H, et al. Interlayer lithium plating in Au nanoparticles pillared reduced graphene oxide for lithium metal anodes[J]. Advanced Functional Materials, 2018, 28(41): 1804133.

[26] Shen L, Shi P R, Hao X G, et al. Progress on lithium dendrite suppression strategies from the interior to exterior by hierarchical structure designs[J]. Small, 2020, 16(26): 2000699.

[27] Kim J Y, Chae O B, Wu M, et al. Extraordinary dendrite-free Li

deposition on highly uniform facet wrinkled Cu substrates in carbonate electrolytes[J]. Nano Energy, 2021, 82: 105736.

[28] Zhao Q, Chen X, Hou W, et al. A facile, scalable, high stability Lithium metal anode[J]. SusMat, 2022, 2(1): 104-112.

[29] Huang X Y, Xue J J, Xiao M, et al. Comprehensive evaluation of safety performance and failure mechanism analysis for lithium sulfur pouch cells[J]. Energy Storage Materials, 2020, 30: 87-97.

[30] Jeong J, Chun J, Lim W G, et al. Mesoporous carbon host material for stable lithium metal anode[J]. Nanoscale, 2020, 12(22): 11818-11824.

[31] Kim J, Lee J, Yun J, et al. Functionality of dual-phase lithium storage in a porous carbon host for lithium-metal anode[J]. Advanced Functional Materials, 2020, 30(15): 1910538.

[32] Li J W, Kong Z, Liu X X, et al. Strategies to anode protection in lithium metal battery: A review[J]. InfoMat, 2021, 3(12): 1333-1363.

[33] Zhang X Q, Jin Q, Nan Y L, et al. Electrolyte structure of lithium polysulfides with anti-reductive solvent shells for practical lithium-sulfur batteries[J]. Angewandte Chemie International Edition, 2021, 133(28): 15631-15637.

[34] Hou L P, Yao N, Xie J, et al. Modification of nitrate ion enables stable solid electrolyte interphase in lithium metal batteries[J]. Angewandte Chemie International Edition, 2022, 61(20): e202201406.

[35] Zhang Q K, Zhang X Q, Hou L P, et al. Regulating solvation structure in nonflammable amide-based electrolytes for long-cycling andsafe lithium metal batteries[J]. Advanced Energy Materials, 2022, 12(24): 2200139.

[36] Li X Y, Feng S, Zhao C X, et al. Regulating lithium salt to inhibit surface gelation on an electrocatalyst for high-energy-density lithium –sulfur batteries[J]. Journal of the American Chemical Society, 2022, 144(32): 14638-14646.

[37] Wang Z, Hou L P, Li Z, et al. Highly soluble organic nitrate additives for practical lithium metal batteries[J]. Carbon Energy, 2023, 5: e283.

[38] Guo F, Chen X, Hou Y H, et al. Improved cycling of Li| | NMC811 batteries under practical conditions by a localized high-concentration electrolyte[J]. Small, 2023, 19: 2207290.

[39] Ye S F, Wang L F, Liu F F, et al. g-C_3N_4 derivative artificial organic/inorganic composite solid electrolyte interphase layer for stable lithium metal anode[J]. Advanced Energy Materials, 2020, 10(44): 2002647.

[40] Beichel W, Skrotzki J, Klose P, et al. An artificial SEI layer based on an inorganic coordination polymer with self-healing ability for long-lived rechargeable lithium-metal batteries[J]. Batteries & Supercaps, 2022, 5(2): e202100347.

[41] Chen C, Liang Q W, Wang G, et al. Grain-boundary-rich artificial SEI layer for high-rate lithium metal anodes[J]. Advanced Functional Materials, 2022, 32(4): 2107249.

[42] Li Z, Hou L P, Zhang X Q, et al. A nafion protective layer for stabilizing lithium metal anodes in working lithium-sulfur batteries[J]. Battery Energy, 2022, 1(3): 20220006.

[43] Zhao F F, Zhai P B, Wei Y, et al. Constructing artificial SEI layer on lithiophilic MXene surface for high-performance lithium metal anodes[J]. Advanced Science, 2022, 9(6): 2103930.

[44] Zhang R, Chen B, Shi C S, et al. Decreasing interfacial pitfalls with self-grown sheet-like Li_2S artificial solid-electrolyte interphase for enhanced cycling performance of lithium metal anode[J]. Small, 2023, 19: 2208095.

[45] Liu B, Zhang Y, Pan G X, et al. Ordered lithiophilic sites to regulate Li plating/stripping behavior for superior lithium metal anodes[J]. Journal of Materials Chemistry A, 2019, 7(38): 21794-21801.

[46] Luo L, Li J Y, Asl H Y, et al. A 3D lithiophilic Mo_2N-modified carbon nanofiber architecture for dendrite-free lithium-metal anodes in a full cell[J]. Advanced Materials, 2019, 31(48): 1904537.

[47] Chen X R, Li B Q, Zhao C X, et al. Synergetic coupling of lithiophilic sites and conductive scaffolds for dendrite-free lithium metal anodes[J]. Small Methods, 2020, 4(6): 1900177.

[48] Wu Q P, Zheng Y J, Guan X, et al. Dynamical SEI reinforced by open-architecture MOF film with stereoscopic lithiophilic sites for high-performance lithium-metal batteries[J]. Advanced Functional Materials, 2021, 31(28): 2101034.

[49] Jeon Y, Kim J, Jang H, et al. Argentophilic pyridinic nitrogen for embedding lithiophilic silver nanoparticles in a three-dimensional carbon scaffold for reversible lithium plating/stripping[J]. Journal of Materials Chemistry A, 2022, 10(4): 1768-1779.

[50] Liu Y H, Sun J M, Hu X Q, et al. Lithiophilic sites dependency of lithium deposition in Li metal host anodes[J]. Nano Energy, 2022, 94: 106883.

[51] Ahn C H, Kim J J, Yang W S, et al. Multiple functional biomolecule-based metal-organic-framework-reinforced polyethylene oxide composite electrolytes for high-performance solid-state lithium batteries[J]. Journal of Power Sources, 2023, 557: 232528.

[52] Cui J, Du Y F, Zhao L, et al. Thermal stable poly-dioxolane based electrolytes via a robust crosslinked network for dendrite-free solid-state Li-metal batteries[J]. Chemical Engineering Journal, 2023, 461: 141973.

[53] Guo Y, Wu S C, He Y B, et al. Solid-state lithium batteries: Safety and prospects[J]. eScience, 2022, 2(2): 138-163.

[54] Wu L Q, Wang Y T, Guo X W, et al. Interface science in polymer-based composite solid electrolytes in lithium metal batteries[J]. SusMat, 2022, 2(3): 264-292.

[55] Zhao T, Kou W J, Zhang Y F, et al. Laminar composite solid electrolyte with succinonitrile-penetrating metal-organic framework (MOF) for stable anode interface in solid-state lithium metal battery[J]. Journal of Power Sources, 2023, 554: 232349.

[56] Wu J Y, Rao Z X, Liu X T, et al. Composite lithium metal anodes with lithiophilic and low-tortuosity scaffold enabling ultrahigh currents and capacities in carbonate electrolytes[J]. Advanced Functional Materials, 2021, 31(14): 2009961.

[57] Chen W Y, Li S P, Wang C H, et al. Targeted deposition in a

lithiophilic silver-modified 3D Cu host for lithium-metal anodes[J]. Energy & Environmental Materials, 2022, https://doi.org/10.1002/eem2.12412.

[58] Liu P, Su H, Liu Y, et al. LiBr-LiF-rich solid-electrolyte interface layer on lithiophilic 3D framework for enhanced lithium metal anode[J]. Small Structures, 2022, 3(6): 2200010.

[59] Yu S C, Wu Z H, Holoubek J, et al. A fiber-based 3D lithium host for lean electrolyte lithium metal batteries[J]. Advanced Science, 2022, 9(10): 2104829.

[60] Hu L, Deng J J, Liang Q H, et al. Engineering current collectors for advanced alkali metal anodes: A review and perspective[J]. EcoMat, 2023, 5(1): e12269.

[61] Liu H R, Zhao M L, Bai X D, et al. An ultrafast rechargeable and high durability lithium metal battery using composite electrolyte with the three-dimensional inorganic framework by $Li_{6.4}La_3Zr_{1.4}Ta_{0.6}O_{12}$ surface functionalization[J]. eTransportation, 2023, 16: 100234.

[62] Ni S Y, Tan S S, An Q Y, et al. Three dimensional porous frameworks for lithium dendrite suppression[J]. Journal of Energy Chemistry, 2020, 44: 73-89.

[63] Liu Y H, Li Y F, Sun J M, et al. Present and future of functionalized Cu current collectors for stabilizing lithium metal anodes[J]. Nano Research Energy, 2023, 2: e9120048.

[64] Jiang Z P, Jin L, Zeng Z Q, et al. Facile preparation of a stable 3D host for lithium metal anodes[J]. Chemical Communications, 2020, 56(68): 9898-9900.

[65] Zhan Y X, Shi P, Zhang X Q, et al. The insights of lithium metal plating/stripping in porous hosts: Progress and perspectives[J]. Energy Technology, 2021, 9(2): 2000700.

[66] Liu F F, Jin Z Z, Hu Z X, et al. Constructing Co_3O_4 nanowires on carbon fiber film as a lithiophilic host for stable lithium metal anodes[J]. Chemistry – An Asian Journal, 2020, 15(7): 1057-1066.

[67] Cha E, Yun J H, Ponraj R, et al. A mechanistic review of lithiophilic materials: Resolving lithium dendrites and advancing lithium metal-based batteries[J]. Materials Chemistry Frontiers, 2021, 5(17): 6294-6314.

[68] Wang J P, Lan D N, Chen G Y, et al. Built-in stable lithiophilic sites in 3D current collectors for dendrite free Li metal electrode[J]. Small, 2022, 18(27): 2106718.

[69] Shi P, Zhang X Q, Shen X, et al. A review of composite lithium metal anode for practical applications[J]. Advanced Materials Technologies, 2020, 5(1): 1900806.

[70] Wang H, Wu J Y, Yuan L X, et al. Stable lithium metal anode enabled by 3D soft host[J]. ACS Applied Materials & Interfaces, 2020, 12(25): 28337-28344.

[71] Zhan Y X, Shi P, Jin C B, et al. Regulating the two-stage accumulation mechanism of inactive lithium for practical composite lithium metal anodes[J]. Advanced Functional Materials, 2022, 32(43): 2206834.

[72] Zhan Y X, Shi P, Zhang R, et al. Deciphering the effect of electrical conductivity of hosts on lithium deposition in composite lithium metal anodes[J]. Advanced Energy Materials, 2021, 11(37): 2101654.

[73] Yun J, Park B K, Won E S, et al. Bottom-up lithium growth triggered by interfacial activity gradient on porous framework for lithium-metal anode[J]. ACS Energy Letters, 2020, 5(10): 3108-3114.

[74] Lai Y M, Zhao Y, Cai W P, et al. Constructing ionic gradient and lithiophilic interphase for high-rate li-metal anode[J]. Small, 2019, 15(47): 1905171.

[75] Fang Y J, Zhang S L, Wu Z P, et al. A highly stable lithium metal anode enabled by Ag nanoparticle –embedded nitrogen-doped carbon macroporous fibers[J]. Science Advances, 2021, 7(21): eabg3626.

[76] Ma Y, Wu F, Chen N, et al. Reversing the dendrite growth direction and eliminating the concentration polarization *via* an internal electric field for stable lithium metal anodes[J]. Chemical Science, 2022, 13(32): 9277-9284.

[77] Lu L L, Ge J, Yang J N, et al. Free-standing copper nanowire network current collector for improving lithium anode performance[J]. Nano Letters, 2016, 16(7): 4431-4437.

[78] Huang S B, Zhang H, Fan L Z. Confined lithium deposition triggered by an integrated gradient scaffold for a lithium-metal anode[J]. ACS Applied Materials & Interfaces, 2022, 14(15): 17539-17546.

[79] Xiang J W, Yuan L X, Shen Y, et al. Improved rechargeability of lithium metal anode via controlling lithium-ion flux[J]. Advanced Energy Materials, 2018, 8(36): 1802352.

[80] Zhou S, Zhang Y F, Chai S M, et al. Incorporation of LiF into functionalized polymer fiber networks enabling high capacity and high rate cycling of lithium metal composite anodes[J]. Chemical Engineering Journal, 2021, 404: 126508.

[81] Tan Y H, Lu G X, Zheng J H, et al. Lithium fluoride in electrolyte for stable and safe lithium-metal batteries[J]. Advanced Materials, 2021, 33(42): 2102134.

[82] Pathak R, Chen K, Wu F, et al. Advanced strategies for the development of porous carbon as a Li host/current collector for lithium metal batteries[J]. Energy Storage Materials, 2021, 41: 448-465.

[83] Zhou J H, Wu F, Wei G L, et al. Lithium-metal host anodes with top-to-bottom lithiophilic gradients for prolonged cycling of rechargeable lithium batteries[J]. Journal of Power Sources, 2021, 495: 229773.

[84] Lang J L, Jin Y, Luo X Y, et al. Surface graphited carbon scaffold enables simple and scalable fabrication of 3D composite lithium metal anode[J]. Journal of Materials Chemistry A, 2017, 5(36): 19168-19174.

[85] Liu L, Yin Y X, Li J Y, et al. Uniform lithium nucleation/growth induced by lightweight nitrogen-doped graphitic carbon foams for high-performance lithium metal anodes[J]. Advanced Materials, 2018, 30(10): 1706216.

[86] Wang A X, Tang S, Kong D B, et al. Bending-tolerant anodes for lithium-metal batteries[J]. Advanced Materials, 2018, 30(1):

1703891.

[87] Chen J Y, Wang Y Z, Li S J, et al. Porous metal current collectors for alkali metal batteries[J]. Advanced Science, 2023, 10(1): 2205695.

[88] Jin S, Sun Z W, Guo Y L, et al. High areal capacity and lithium utilization in anodes made of covalently connected graphite microtubes[J]. Advanced Materials, 2017, 29(38): 1700783.

[89] Ye H, Xin S, Yin Y X, et al. Stable Li plating/stripping electrochemistry realized by a hybrid Li reservoir in spherical carbon granules with 3D conducting skeletons[J]. Journal of the American Chemical Society, 2017, 139(16): 5916-5922.

[90] Yang Y, Zhao M, Geng H B, et al. Three-dimensional graphene/Ag aerogel for durable and stable Li metal anodes in carbonate-based electrolytes[J]. Chemistry-A European Journal, 2019, 25(19): 5036-5042.

[91] Mao H, Yu W, Cai Z Y, et al. Current-density regulating lithium metal directional deposition for long cycle-life Li metal batteries[J]. Angewandte Chemie International Edition, 2021, 60: 19306.

[92] Park S, Jin H J, Yun Y S. Advances in the design of 3D-structured electrode materials for lithium-metal anodes[J]. Advanced Materials, 2020, 32(51): 2002193.

[93] Guan W Q, Hu X Q, Liu Y H, et al. Advances in the emerging gradient designs of Li metal hosts[J]. Research, 2022, 2022: 9846537.

[94] Chen X R, Chen X, Yan C, et al. Role of lithiophilic metal sites in lithium metal anodes[J]. Energy & Fuels, 2021, 35(15): 12746-12752.

[95] Chen X R, Zhao B C, Yan C, et al. Review on Li deposition in working batteries: from nucleation to early growth[J]. Advanced Materials, 2021, 33(8): 2004128.

[96] Zhang H M, Liao X B, Guan Y P, et al. Lithiophilic-lithiophobic gradient interfacial layer for a highly stable lithium metal anode[J]. Nature Communications, 2018, 9(1): 3729.

[97] Yan X L, Zhang Q F, Xu W J, et al. Bottom-top channeling Li nucleation and growth by a gradient lithiophilic 3D conductive host for highly stable Li-metal anodes[J]. Journal of Materials Chemistry A, 2020, 8(4): 1678-1686.

[98] Yun J, Shin H R, Won E S, et al. Confined Li metal storage in porous carbon frameworks promoted by strong Li-substrate interaction[J]. Chemical Engineering Journal, 2022, 430: 132897.

[99] Lin D, Liu Y, Liang Z, et al. Layered reduced graphene oxide with nanoscale interlayer gaps as a stable host for lithium metal anodes[J]. Nature Nanotechnology, 2016, 11(7): 626-632.

[100] Chen H, Pei A, Wan J Y, et al. Tortuosity effects in lithium-metal host anodes[J]. Joule, 2020, 4(4): 938-952.

[101] Huang Q K, Ni S Y, Jiao M L, et al. Aligned carbon-based electrodes for fast-charging batteries: a review[J]. Small, 2021, 17(48): 2007676.

[102] Ni S Y, Sheng J Z, Zhang C, et al. Dendrite-free lithium deposition and stripping regulated by aligned microchannels for stable lithium metal batteries[J]. Advanced Functional Materials, 2022, 32(21): 2200682.

[103] Wang G, Xiong X H, Zou P J, et al. Lithiated zinc oxide nanorod arrays on copper current collectors for robust Li metal anodes[J]. Chemical Engineering Journal, 2019, 378: 122243.

[104] Tantratian K, Cao D X, Abdelaziz A, et al. Stable Li metal anode enabled by space confinement and uniform curvature through lithiophilic nanotube arrays[J]. Advanced Energy Materials, 2020, 10(5): 1902819.

[105] Zhu Z X, Liu B, Qian Y, et al. Spatially distributed lithiophilic gradient in low-tortuosity 3D hosts via capillary action for high-performance Li metal anodes[J]. Advanced Energy Materials, 2022, 13(7): 2203687.

[106] Cao W Z, Chen W M, Lu M, et al. In situ generation of Li_3N concentration gradient in 3D carbon-based lithium anodes towards highly-stable lithium metal batteries[J]. Journal of Energy Chemistry, 2023, 76: 648-656.

[107] Hong S H, Jung D H, Kim J H, et al. Electrical conductivity gradient based on heterofibrous scaffolds for stable lithium-metal batteries[J]. Advanced Functional Materials, 2020, 30(14): 1908868.

[108] Li J, Zou P C, Chiang S W, et al. A conductive-dielectric gradient framework for stable lithium metal anode[J]. Energy Storage Materials, 2020, 24: 700-706.

[109] Zou P C, Chiang S W, Zhan H C, et al. A periodic "self-correction" scheme for synchronizing lithium plating/stripping at ultrahigh cycling capacity[J]. Advanced Functional Materials, 2020, 30(21): 1910532.

[110] Sun B, Zhang Q, Xu W L, et al. A gradient topology host for a dendrite-free lithium metal anode[J]. Nano Energy, 2022, 94: 106937.

[111] Sun X J, Shao C Z, Zhang F, et al. SiC nanofibers as long-life lithium-ion battery anode materials[J]. Frontiers in Chemistry, 2018, 6: 166.

[112] Zhou S, Fu C Y, Chang Z, et al. Conductivity gradient modulator induced highly reversible Li anodes in carbonate electrolytes for high-voltage lithium-metal batteries[J]. Energy Storage Materials, 2022, 47: 482-490.

[113] Pu J, Li J C, Zhang K, et al. Conductivity and lithiophilicity gradients guide lithium deposition to mitigate short circuits[J]. Nature Communications, 2019, 10(1): 1896.

[114] Cai Q C, Qin X Y, Lin K, et al. Gradient structure design of a floatable host for preferential lithium deposition[J]. Nano Letters, 2021, 21(24): 10252-10259.

[115] Guo B K, Shu J, Wang Z X, et al. Electrochemical reduction of nano-SiO_2 in hard carbon as anode material for lithium ion batteries[J]. Electrochemistry Communications, 2008, 10(12): 1876-1878.

[116] Lai L S, Yeong Y F, Ani N C, et al. Effect of synthesis parameters on the formation of zeolitic imidazolate framework 8 (ZIF-8) nanoparticles for CO_2 adsorption[J]. Particulate Science and Technology, 2014, 32(5): 520-528.

[117] Shi Y B, Yang S H, Sun X R, et al. Metal-organic framework

derived gradient interfacial layer for stable lithium metal anode[J]. Electrochimica Acta, 2022, 417: 140333.

[118] Chen H, Yang Y F, Boyle D T, et al. Free-standing ultrathin lithium metal-graphene oxide host foils with controllable thickness for lithium batteries[J]. Nature Energy, 2021, 6(8): 790-798.

[119] Lin L D, Qin K, Hu Y S, et al. A better choice to achieve high volumetric energy density: anode-free lithium-metal batteries[J]. Advanced Materials, 2022, 34(23): 2110323.

[120] Yu Z, Yang Q Y, Xue W J, et al. Uniformizing the lithium deposition by gradient lithiophilicity and conductivity for stable lithium-metal batteries[J]. Nanoscale, 2023, 15(9): 4529-4535.

[121] Shen X, Zhang R, Shi P, et al. How does external pressure shape Li dendrites in Li metal batteries?[J]. Advanced Energy Materials, 2021, 11(10): 2003416.

[122] Liu H, Sun X, Cheng X B, et al. Working principles of lithium metal anode in pouch cells[J]. Advanced Energy Materials, 2022, 12(47): 2202518.

[123] Noh H J, Lee M H, Kim B G, et al. 3D carbon-based porous anode with a pore-size gradient for high-performance lithium metal batteries[J]. ACS Applied Materials & Interfaces, 2021, 13(46): 55227-55234.

[124] Liu H, Di J, Wang P, et al. A novel design of 3D carbon host for stable lithium metal anode[J]. Carbon Energy, 2022, 4(4): 654-664.

[125] Zhan Y X, Shi P, Ma X X, et al. Failure mechanism of lithiophilic sites in composite lithium metal anode under practical conditions[J]. Advanced Energy Materials, 2022, 12(2): 2103291.